Quantum state of hydrogen in $LaNi_5$

Tomoaki Kaneko, Akinori Tezuka, Hiroshi Ogawa, and Tamio Ikeshoji*
Research Institute for Computational Sciences (RICS), National Institute of Advanced Industrial Science and Technology (AIST), AIST Tsukuba Central 2, Umezono 1-1-1, Tsukuba 305-8568, Japan
(Received 20 January 2010; published 20 May 2010)

The quantum state of the hydrogen atom that is trapped at the most stable octahedral interstitial site in the $LaNi_5$ crystal is determined. A three-dimensional potential-energy surface for the hydrogen atom around the 3*f* site is obtained by applying first-principles electronic-structure calculations. The time-independent Schrödinger equation for the hydrogen atom under the potential obtained is solved. The hydrogen wave function distributes over the neighboring sites, 6*i*-3*f*-6*i*, that have been proposed by various workers so far. The energy spectra of the hydrogen atom well explain those of inelastic neutron scattering.

DOI: 10.1103/PhysRevB.81.184302 PACS number(s): 61.72.S−, 71.15.−m, 61.05.F−

I. INTRODUCTION

$LaNi_5$ and its related alloys have attracted considerable interest for hydrogen storage materials because of their rapid hydrogen absorption and desorption rate and higher capacity of hydrogen per volume than liquid hydrogen.[1,2] Due to the small mass of the hydrogen atom, the typical zero-point energy in metals can become larger than the thermal energy, and the spatial distribution of zero-point oscillation exceeds the thermal distribution. Therefore, the quantum-mechanical feature of the hydrogen atom is not negligible and plays an important role even at room temperature. The purpose of this study is to clarify the role of the quantum-mechanical features of the hydrogen atom in $LaNi_5$ and its effect on neutron scattering.

When the hydrogen atom is absorbed in the metal, it occupies an interstitial site and causes lattice distortion, which in turn decreases the total energy of the system. In this case, the translational symmetry of the host crystal is broken and the hydrogen is not in the Bloch state. The energy supplement is needed to move such hydrogen atoms to the other sites even in the case of quantum tunneling. Then, the hydrogen exists in a so-called self-trapped state,[3] which is a stable state; hence, the hydrogen cannot move to other sites if the coupling between the phonon and the hydrogen local oscillation is negligible. For this hydrogen, typical excitation energies are considerably larger than the phonon energy due to the light mass of hydrogen. Therefore, the hydrogen behaves as a decoupled oscillator from lattice phonon.

$LaNi_5$ has a hexagonal lattice structure ($CaCu_5$ structure, space group $P6/mmm$), which is characterized by primitive vectors $\boldsymbol{a}$, $\boldsymbol{b}$, and $\boldsymbol{c}$ with $|\boldsymbol{a}|=|\boldsymbol{b}|$, $\boldsymbol{a}\perp\boldsymbol{c}$, and $\boldsymbol{b}\perp\boldsymbol{c}$, as shown in Fig. 1(a). In $LaNi_5$, there are many hydrogen sites, which exhibit considerably high capacity of hydrogen. According to the neutron-diffraction experiments that are based on the Rietveld refinement, the most stable site of hydrogen in the solid solution phase is the La_2Ni_4 octahedral interstitial site.[4–7] Most of the first-principles calculations[8–11] also support the stability of the octahedral site, while Nakamura *et al.*[12] proposed La_2Ni_2 tetrahedral site. However, determining the exact hydrogen position in the octahedral site is a difficult task.

The 3*f* site, which is given by (0.5, 0, 0) in a fractional coordinate with $\boldsymbol{a}$, $\boldsymbol{b}$, and $\boldsymbol{c}$, was suggested by Fischer *et al.*,[4] 12*n* site, which is given by (0.455, 0, 0.11), was suggested by Soubeyroux *et al.*,[5] and 6*i* site, which is given by (0.5, 0, 0.09), was suggested by Kisi *et al.*[7] These sites are located on a plane spanned by vectors $\boldsymbol{a}$ and $\boldsymbol{c}$, as shown in Fig. 1(b). According to the two-dimensional potential surface on the plane calculated by Tezuka *et al.*,[11] the hydrogen should be extended around two 6*i* due to quantum fluctuation because the height of the potential barrier between neighboring *i*-*i* sites is too small to confine hydrogen in a single site.

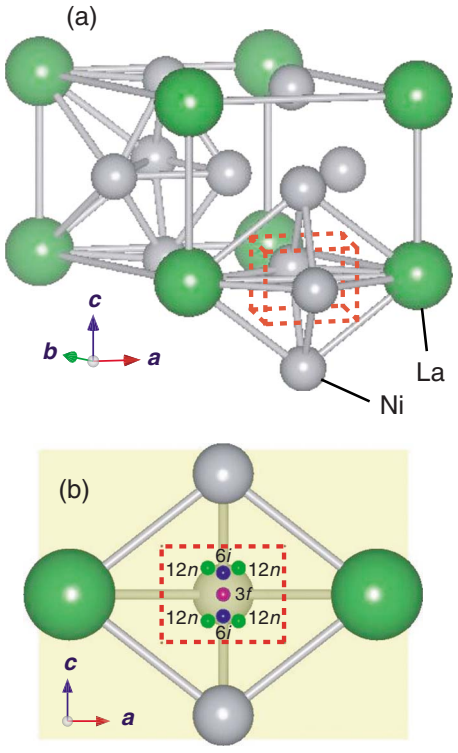

FIG. 1. (Color online) (a) Crystal structure of $LaNi_5$. Two Ni atoms are added outside of the unit cell to show the calculation region (box of red dashed lines). The most stable hydrogen site, the La_2Ni_4 octahedral interstitial site, is located in the box. (b) The octahedral interstitial site in a plane spanned by vectors $\boldsymbol{a}$ and $\boldsymbol{c}$. Various hydrogen sites, 3*f*, 12*n*, and 6*i*, proposed in Refs. 4–7 are presented by the different colors.

In this study, the three-dimensional potential-energy surface for the self-trapped hydrogen is calculated by applying first-principles electronic-structure calculations. By using this potential, the wave-function and energy eigenvalues of a single hydrogen atom are calculated. The quantum-mechanical feature which will be observed on neutron-scattering experiments is predicted. In this paper, we shall focus on the hydrogen in the solid solution phase, $LaNi_5H_n$ ($n<1$). This paper is organized as follows: the details of calculations are provided in Sec. II. The results of potential-energy surface, energy eigenvalues and wave functions of hydrogen atom, and pair-distribution functions are presented in Sec. III. A short summary is provided in Sec. IV.

II. COMPUTATIONAL DETAILS

In this study, the first-principles calculations based on the density-functional theory (DFT) for electronic structures were used to calculate the potential energy of the hydrogen atom. We employed the quantum materials simulator (QMAS) code,[13] which uses the projector augmented wave method.[14] Perdew-Burke-Ernzerhof (PBE) version general gradient approximation[15] was chosen as the exchange-correlation term. We introduced one hydrogen atom inside the La_2Ni_4 octahedral interstitial site in $1\times1\times2$ supercell of $LaNi_5$ and performed the geometrical optimization (for atom positions and lattice constants) with imposing the hexagonal lattice structure. The cut-off energy for the plane-wave basis and the number of k points in the Brillouin zone were chosen to be 680 eV (50 Ry) and 288 ($6\times6\times8$), respectively. For this supercell, we obtained the lattice constant as $a=5.057$ Å and $c=7.941$ Å. The most stable position of hydrogen was obtained in the octahedral $6i$ site, which is given by (0.5, 0, 0.0265) in the fractional coordinate. Note that the fractional coordinate in the $\boldsymbol{c}$ direction is given by c of the supercell. From hereafter, fractional coordinates with c are used.

According to the adiabatic approximation in the electronic-structure calculations, the electronic state can follow the change in the nuclear position instantaneously. This approximation is based on the fact that the considerable difference in the time scale between the electronics state and the nuclear state comes from considerable difference in the mass between them. The nuclei are assumed as charged point particles and the individual electron's position is eliminated from the nuclear dynamics. We shall use the corresponding approximation for the hydrogen and the heavy-nuclear (La and Ni) states, i.e., the hydrogen atom can instantaneously adjust to the change in the position of the heavy nucleus. As mentioned previously, hydrogen causes lattice distortion and exists in the stable self-trapped state. Thus, the hydrogen atom is confined and moves rapidly in the distorted and rigid lattice. In order to handle the hydrogen quantum state, the hydrogen potential energy was calculated from the total electronic energy. It was obtained by placing a hydrogen atom on a regular grid point in the vicinity of the $6i$ site without the further optimization of the La and Ni positions, which are fixed at the geometry optimized structure with the hydrogen atom introduced at the $6i$ site.

Let $\boldsymbol{R}_\mathrm{H}$ be a classical position of a hydrogen atom and $E_{La_2Ni_{10}H}(\boldsymbol{R}_\mathrm{H})$ be the total energy of the $La_2Ni_{10}H$ with hydrogen located at $\boldsymbol{R}_\mathrm{H}$. A systematic DFT calculation for various hydrogen atom positions was performed to obtain $E_{La_2Ni_{10}H}(\boldsymbol{R}_\mathrm{H})$ as described in the above section. In this study, we shall measure the potential energy from that at the potential bottom, i.e., the total energy obtained after the geometry optimization. Therefore, the potential for self-trapped hydrogen becomes

$$V(\boldsymbol{R}_\mathrm{H}) = E_{La_2Ni_{10}H}(\boldsymbol{R}_\mathrm{H}) - E_{La_2Ni_{10}H}(\boldsymbol{R}_\mathrm{H}^0), \tag{1}$$

where $\boldsymbol{R}_\mathrm{H}^0$ is the hydrogen position at the potential minimum.

Let X, Y, and Z axes be along $\boldsymbol{a}$, $\boldsymbol{a}/6+\boldsymbol{b}/3$, and $\boldsymbol{c}$, respectively. Then, the hydrogen coordinate can be written in the orthogonal coordinates, X, Y, and Z, of these vectors as follows:

$$\boldsymbol{R}_\mathrm{H} = X\boldsymbol{a} + Y\left(\frac{\boldsymbol{a}}{6}+\frac{\boldsymbol{b}}{3}\right) + Z\boldsymbol{c}. \tag{2}$$

The origin is chosen at the $3f$ site. We calculated the three-dimensional potential surface in $-0.2\le X\le0.2$, $-0.6\le Y\le0.6$, and $-0.1\le Z\le0.1$. The calculated points are in the intervals 0.05 (0.253 Å) for X, 0.2 (0.292 Å) for Y, and 0.025 (0.198 Å) for Z. The region in which the potential-energy calculation was performed is indicated by the box shown as dashed (red) lines in Fig. 1(a).

By using this three-dimensional potential surface, we constructed the Hamiltonian matrix by discretized representation. In such a representation, the potential part is given by a diagonal matrix, while the kinetic-energy part is not. To construct the kinetic-energy matrix, we used the appropriate complete orthonormal basis set. In this study, we chose the basis set as the plane-wave solutions in the orthorhombic cell under the periodic boundary conditions and the wave function of the three-dimensional infinite height well potential. In this representation, the Hamiltonian can be written in the real symmetric matrix and the wave functions are given by real functions. Then, the time-independent Schrödinger equation of the hydrogen atom was given by the eigenvalue problem of the Hamiltonian matrix and was solved numerically.

In this calculation, we confirmed that the dependence of the energy eigenvalues on the choice of the basis set was sufficiently small (in the order of 0.1 meV) for several lower states. This indicates that the wave function does not reach the boundary and the hydrogen is confined in the calculated region for the quantum treatment. Furthermore, we confirmed that the change in energy eigenvalue for the several lower states are also small with the increase in the grid number of the interpolation for the potential energy. This means that the grid size is sufficiently small.

III. RESULTS AND DISCUSSION

A. Wave function of hydrogen and energy eigenvalue

Figures 2(a) and 2(b) show the calculated potential-energy profiles at $Y=0$ and $X=0$, respectively, for the self-trapped hydrogen. If we treat the hydrogen as a point particle, the hydrogen site becomes $6i$, which is given by (0.5, 0, 0.0265) in the fractional coordinate with $\boldsymbol{a}$, $\boldsymbol{b}$, and $\boldsymbol{c}$. The deviation of the H position from the La plane (0.21 Å) is much smaller

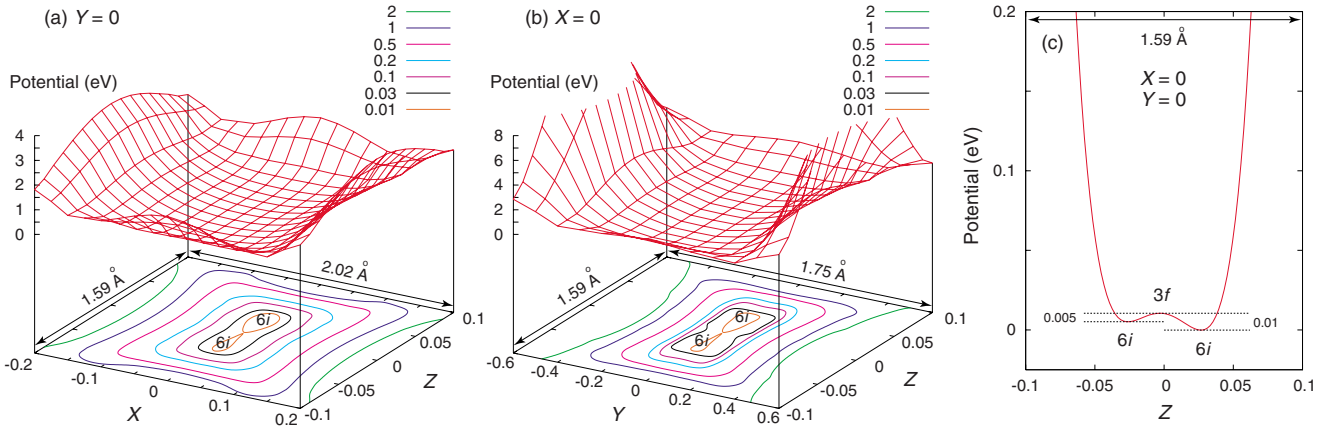

FIG. 2. (Color online) Calculated potential-energy profiles (a) on the X-Z surface at $Y=0$, (b) on the Y-Z surface at $X=0$, and (c) in the Z direction on $X=0$ and $Y=0$. The hydrogen atom is classically self-trapped in the upper $6i$ site. The potential in the Y direction is narrower than the widths in others. We used the fractional coordinate defined by Eq. (2).

than that obtained by inserting a hydrogen atom in a primitive $LaNi_5$ cell (0.34 Å without cell optimization and 0.37 Å with cell optimization).[11] In our calculation, the degree of freedom in the relaxation of the Ni position located in the plane spanned by $\boldsymbol{a}$ and $\boldsymbol{c}$ becomes larger with the increase in the calculation cell size. Another local minimum can be found at around $(0.5,0,-0.03)$ in the fractional coordinate with $\boldsymbol{a}$, $\boldsymbol{b}$, and $\boldsymbol{c}$. Figure 2(c) shows the potential energy on the line of $X=0$ and $Y=0$ including two $6i$ sites with a small barrier in between. The barrier height from the hydrogen trapped $6i$ site is 0.01 eV and is considerably smaller than the typical zero-point energy of hydrogen as we shall see below.

The potential valley in the Y direction is narrow and that in the Z direction is relatively wide as we can see in Figs. 2(a) and 2(b). The width at $V(\boldsymbol{R}_H)=0.1$ eV is 0.5 Å in the X direction, 0.3 Å in the Y direction, and 0.8 Å in the Z direction. The nearest atom from the center of the octahedral, $3f$, is Ni at (2/3, 1/3, 0) in the fractional coordinate with $\boldsymbol{a}$, $\boldsymbol{b}$, and $\boldsymbol{c}$. This atomic configuration leads to the narrow potential in the Y direction. Thus, the potential is a tilted double well with strong anisotropy.

Figure 3 shows the calculated wave function of the (a) hydrogen atom and (b) deuterium atom. The calculated potential has parity in the X and Y directions, i.e.,

$$V(-X,Y,Z)=V(X,-Y,Z)=V(X,Y,Z). \tag{3}$$

Therefore, the wave functions are the eigenstate of parity in the X and Y directions. Even in the ground state, the wave function is not localized in a single $6i$ site and spreads over the adjacent $6i$ sites. The oscillation modes in the Z direction are more easily excited when compared with the other directions because the potential valley in the Z direction is wider than the potential valleys in other directions. Due to the narrow potential in the Y direction, the energy eigenvalue of the oscillation mode in the Y direction is higher than that in other directions.

The obtained energy eigenvalues are summarized in Table I. The corresponding zero-point energy is 0.144 eV for H and 0.088 eV for D. Due to the strong anisotropy, the energy difference between the first excited state and the ground state is smaller than the zero-point energy. An activation energy from the $6i$ site to the $LaNi_3$ tetrahedral $12o$ site is 0.3–0.4 eV.[11,17] Thus, it is not sufficient for the decrease in the activation energy when compared to the thermal energy at room temperature. For the hydrogen-diffusion process, quantum-mechanical effects such as tunneling should play an important role at low temperature.

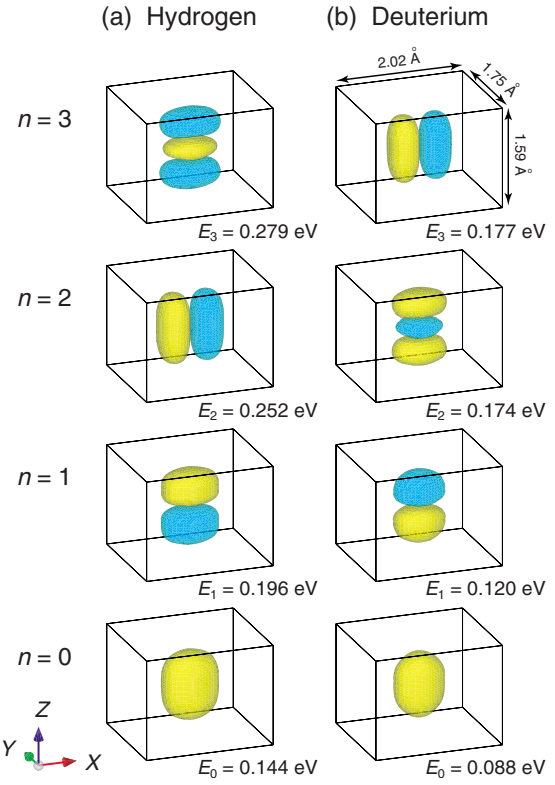

FIG. 3. (Color online) Isovalue surface of the calculated wave function for (a) hydrogen atom and (b) deuterium atom from the ground state ($n=0$, bottom panel) to the third excited state ($n=3$, top panel). The different color represents the different sign in the wave function.

TABLE I. Calculated energy eigenvalues of hydrogen and deuterium atoms at the nth state (in eV).

n	H	D
0	0.144	0.088
1	0.196	0.120
2	0.252	0.174
3	0.279	0.177

The zero-point energy can be also estimated in the harmonic approximation. To obtain the frequency of the oscillation, we calculated the potential energy on the lines parallel to the axes including the potential minimum with finer grid (0.01 for X, 0.02 for Y, and 0.005 for Z). Then, we fitted the potential surface to the three-dimensional parabolic curve as follows:

$$V(\boldsymbol{R}_{\mathrm{H}}) = \frac{1}{2}M \sum_{i=X,Y,Z} \omega_i^2 q_i^2, \tag{4}$$

where M is the mass of hydrogen or deuterium, q_i is displacement from the potential minimum in the i direction, and ω_i is the angular frequency. The zero-point energy is given by

$$E_0 = \frac{\hbar}{2}(\omega_X + \omega_Y + \omega_Z), \tag{5}$$

and the results for hydrogen and deuterium are summarized in Table II. The zero-point energies calculated in the harmonic approximation are larger than those calculated by solving the Schördinger equation. Although the potential surface is parabolic around the vicinity of the potential minimum, the hydrogen atom extends to the region where the parabolic approximation is not valid. Furthermore, for the Z-direction excited states, the energy interval between the next higher state becomes larger when the excited state becomes higher. These results indicate that simple harmonic approximation is not applicable for this system.

B. Hydrogen energy spectrum

The energy spectrum of the hydrogen atom has been measured with inelastic neutron-scattering experiment.[16,18] In this experiment, hydrogen rather than deuterium was used because the incoherent-scattering cross-section of hydrogen

TABLE II. Calculated zero-point energy in each direction and the total zero-point energy within harmonic approximation around the potential minimum (in eV).

	H	D
$\hbar\omega_X/2$	0.050	0.035
$\hbar\omega_Y/2$	0.088	0.062
$\hbar\omega_Z/2$	0.045	0.032
E_0	0.183	0.130

TABLE III. Some level intervals of hydrogen in the low-level region (in meV). The second column shows the direction of $\boldsymbol{Q}$ in which the peak will be observed by the inelastic neutron scattering.

	ΔE	Direction of $\boldsymbol{Q}$
$0\rightarrow1$	52	$\boldsymbol{Q}\parallel\boldsymbol{c}$
$0\rightarrow2$	108	$\boldsymbol{Q}\perp\boldsymbol{c}$
$0\rightarrow3$	135	$\boldsymbol{Q}\parallel\boldsymbol{c}$
$1\rightarrow2$	56	
$1\rightarrow3$	83	$\boldsymbol{Q}\parallel\boldsymbol{c}$

is larger than that of deuterium. The calculated level intervals ΔE for hydrogen in the lower levels are given in Table III. Let $\psi_i(\boldsymbol{R})$ and $\psi_f(\boldsymbol{R})$ be the initial state and the final state of the hydrogen wave function on the scattering event, respectively. Because the interaction between a neutron and a nucleus is described by a delta function, the transition probability between these states by inelastic neutron scattering is proportional to the following quantity under the lowest Born approximation:[3]

$$\left| \int d\boldsymbol{R}\psi_f^*(\boldsymbol{R})\psi_i(\boldsymbol{R})e^{i\boldsymbol{Q}\cdot\boldsymbol{R}} \right|^2 \equiv A(\boldsymbol{Q}), \tag{6}$$

where $\hbar\boldsymbol{Q}=\hbar(\boldsymbol{k}_i-\boldsymbol{k}_f)$ is the momentum transferred from a neutron by scattering with the initial-state wave vector $\boldsymbol{k}_i$ and the final one $\boldsymbol{k}_f$.

Figure 4 shows the calculated $A(\boldsymbol{Q})$ for several $\boldsymbol{Q}$ directions. $A(\boldsymbol{Q})$ vanishes at $Q=0$ due to the absence of the effect on the scattering and starts to increase with Q. In the experiments, possible Q is in 2–10 Å^{-1}. From this figure, excitation $0\rightarrow2$ (108 meV) should be observed for $\boldsymbol{Q}\perp\boldsymbol{c}$ and $0\rightarrow1$ (52 meV), $0\rightarrow3$ (135 meV), and $1\rightarrow3$ (83 meV) for $\boldsymbol{Q}\parallel\boldsymbol{c}$. In Fig. 4(b), we cannot find practical transition for $\boldsymbol{Q}\parallel\boldsymbol{a}+2\boldsymbol{b}$ because of the absence of the y-direction mode in the lower states. Even in this case, however, $\boldsymbol{Q}\parallel2\boldsymbol{a}+\boldsymbol{b}$ and $\boldsymbol{a}+\boldsymbol{b}$ contribution is found because there are rotationally equivalent octahedral sites by 60° and 120°.

These calculated $A(\boldsymbol{Q})$ values are strongly dependent on $\boldsymbol{Q}$. Therefore, the analysis of $\boldsymbol{Q}$ dependence of the spectra can provide further information for determining the hydrogen oscillation mode. For example, $A(\boldsymbol{Q})$ for $0\rightarrow3$ transition is considerably smaller than that for $0\rightarrow1$ in the region $Q<5$ Å^{-1} for $\boldsymbol{Q}\parallel\boldsymbol{c}$. If we choose around $Q\simeq2$ Å^{-1}, $0\rightarrow3$ excitation is suppressed and only $0\rightarrow1$ excitation should be found in the spectra.

Schönfeld *et al.*[18] performed inelastic neutron scattering in a single crystal α-$La^{60}Ni_5H_{0.12}$ at 296 K. In their experiments, corresponding Q range is 5–10 Å^{-1}. At this temperature, the occupation of the first-excited state is estimated as 11% and excitation from $n=1$ should be observed when the transition probability is considerably larger than that from $n=0$. They observed the excitation energy at 98 and 118 meV for $\boldsymbol{Q}\perp\boldsymbol{c}$ and at 55 and 129 mV for $\boldsymbol{Q}\parallel\boldsymbol{c}$. Their results for $\boldsymbol{Q}\parallel\boldsymbol{c}$ (55 and 129 meV) can be understood as the transition $0\rightarrow1$ (52 meV) and $0\rightarrow3$ (135 meV) obtained by the calculation. The transition $1\rightarrow3$ (83 meV) is suppressed due

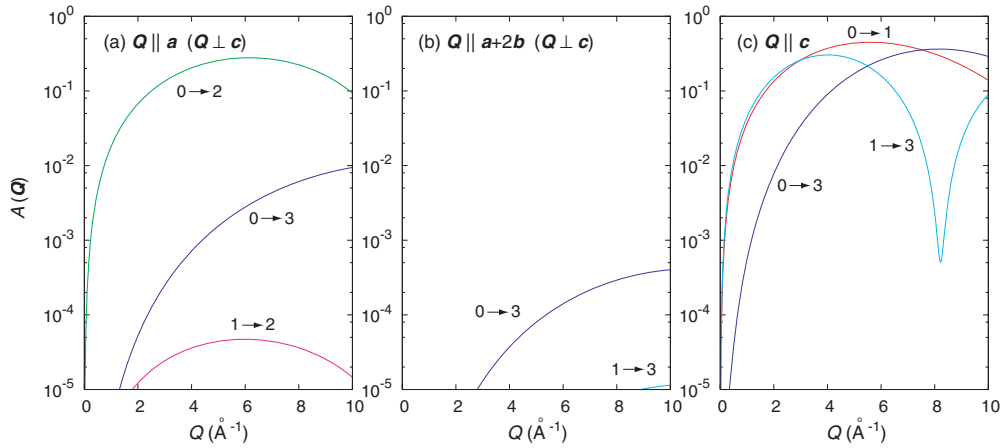

FIG. 4. (Color online) Calculated $A(\boldsymbol{Q})$ as a function of Q for three directions. (a) $\boldsymbol{Q}\|\boldsymbol{a}$, (b) $\boldsymbol{Q}\|\boldsymbol{a}+2\boldsymbol{b}$, and (c) $\boldsymbol{Q}\|\boldsymbol{c}$.

to the low occupation of $n=1$ state and the small scattering probability in the practical Q range. One of two measured peaks for $\boldsymbol{Q}\perp\boldsymbol{c}$ (98 and 118 meV) is corresponding to excitation $0\rightarrow 2$ (108 meV) by the calculation. By considering the symmetry of the wave function, they interpreted that these two observed peaks (98 and 118 meV) for $\boldsymbol{Q}\perp\boldsymbol{c}$ are transition to the X- and Y-directional oscillation modes. However, the energy eigenvalue of the Y-directional oscillation mode is larger than the third excitation state.

Although scattering on another sites ($12o$, $6m$, or $4h$) may contribute to the spectra as predicted by Hempelmann *et al.*[16] from inelastic neutron-scattering measurement for α-$LaNi_5H_{0.15}$ at 423 K; they observed peaks at 57 ± 3, 120 ± 4, 165 ± 5 meV, etc., these assignments are still uncertain due to the occupation problem at hydrogen sites. First-principles calculations so far by different authors give the different stability for each site.[8–12] Even though these points have remained unresolved, our results well explain the experimental spectra.

C. Pair-distribution function

As mentioned previously, the neutron-diffraction experiment with the Rietveld refinement concludes that the most stable hydrogen position in the solid solution phase is in the La_2Ni_4 octahedral site and determining the atomic position has been difficult. In the Rietveld analysis, a Gaussian hydrogen wave function was assumed. For these experiments, a deuterium atom is used instead of the hydrogen atom due to the larger coherent scattering cross-section.

In total neutron-scattering experiments, one can measure a pair-distribution function, which is defined as[19]

$$g_{ij}(r)=\frac{\Delta n_{ij}}{4\pi r^2\rho_j\Delta r}, \tag{7}$$

where $\Delta n_{ij}(r)$ is the number of particles of type j between distance $r-\Delta r/2$ and $r+\Delta r/2$ from the particles of i, and ρ_j is the average density of the particle of type j. Figure 5 shows the calculated pair-distribution function for (a) La-H and La-D and for (b) Ni-H and Ni-D. In this calculation, the wave function of the ground-state hydrogen or deuterium atom was used. In this figure, the vertical (pink) lines represent the pair-distribution function for the fixed atomic configuration and the dashed (blue) curve represents that using the isotropic Gaussian function on a potential minimum ($6i$) with the width 0.2 Å of which the width is estimated from the zero-point energy. Thus, the dashed (blue) curve can be understood as the pair-distribution function after the Rietveld refinement of the hydrogen position. For both H and D, a small difference is observed in the pair-distribution function from that of the Gaussian case. If we use the anisotropic Gaussian function in the analysis, this difference may become smaller than that for the isotropic Gaussian case. Furthermore, because of the practical resolution of r in the total neutron-scattering experiment and the thermal oscillation of the host lattice, such a small difference may not be measurable.

Figure 6 shows the wave-function profiles of the ground-state hydrogen shown in Fig. 3 on the $Y=0$ plane for (a)

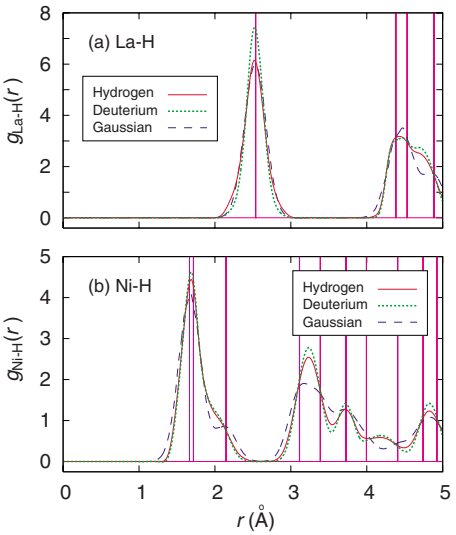

FIG. 5. (Color online) Calculated pair-distribution functions for (a) La-H(D) and for (b) Ni-H(D). The dashed blue curve represents the pair-distribution function when the isotropic Gaussian function is located on the potential minimum ($6i$) instead of the wave function.

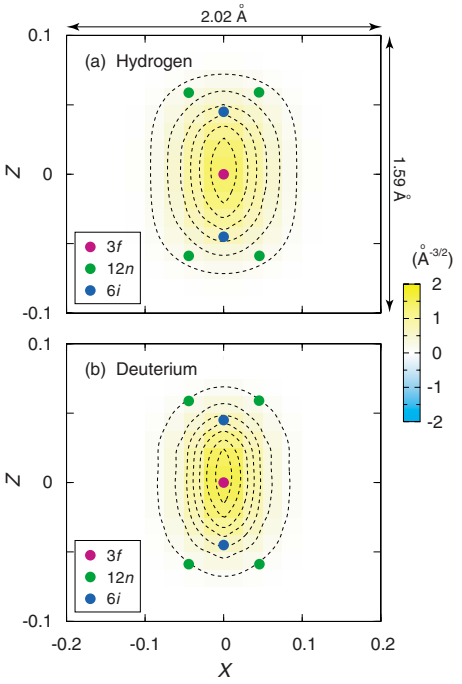

FIG. 6. (Color online) The wave-function profiles of the ground-state hydrogen on the $Y=0$ plane, (a) for hydrogen and (b) for deuterium.

hydrogen and for (b) deuterium. In this figure, the hydrogen sites obtained by neutron diffraction ($3f$, $6i$, and $12n$) are shown in the circles. The wave functions extend these hydrogen sites, suggesting that further refinement of the hydrogen position is difficult, in principle. Such wide distribution of the hydrogen atom may cause experimental ambiguity in determining the detailed hydrogen position. Therefore, the quantum effect of the hydrogen atom is important for understanding the neutron-scattering measurements.

IV. SUMMARY

In this study, the three-dimensional potential-energy surface for a self-trapped hydrogen in the $6i$ site of $LaNi_5$ was obtained by applying first-principles calculations. By using this potential surface, the energy eigenvalues and the wave functions of the self-trapped hydrogen atom in this potential were calculated. The obtained level interval in energy of hydrogen well explain those of inelastic neutron scattering. The directional dependence of the transition between the states is also consistent with the experimental observation. The hydrogen atom is not localized in a single $6i$ site; the hydrogen atom is self-trapped in $6i$ and spreads over several sites ($3f$, $6i$, and $12n$) in the La_2Ni_4 octahedral interstitial site.

ACKNOWLEDGMENTS

This work is supported by New Energy and Industrial Technology Development Organization (NEDO) under "Advanced Fundamental Research on Hydrogen Storage Materials." First-principles calculations were performed on AIST Super Cluster by using QMAS (Quantum MAterials Simulator) developed by Ishibashi *et al.*

*Present address: New Industry Creation Hatchery Center (NICHe), Tohoku University, 6-6-10 Aoba, Aramaki, Aoba-ku, Sendai 980-8579, Japan.

[1] J. H. N. van Vucht, F. A. Kuijpers, and H. C. A. M. Bruning, Philips Res. Rep. **25**, 133 (1970).
[2] J. J. G. Willems and K. H. J. Buschow, J. Less-Common Met. **129**, 13 (1987).
[3] Y. Fukai, *The Metal-Hydrogen System* (Springer-Verlag, Berlin, 1993).
[4] A. Fischer, A. Furrer, G. Busch, and L. Schlapbach, Helv. Phys. Acta **50**, 421 (1977).
[5] J. L. Soubeyroux, A. Percheron-Guegan, and J. C. Achard, J. Less-Common Met. **129**, 181 (1987).
[6] H. Hayakawa, K. Nomura, Y. Ishido, E. Akiba, and S. Shin, J. Less-Common Met. **143**, 315 (1988).
[7] E. H. Kisi, E. M. A. Gray, and S. J. Kennedy, J. Alloys Compd. **216**, 123 (1994).
[8] K. Tatsumi, I. Tanaka, H. Inui, K. Tanaka, M. Yamaguchi, and H. Adachi, Phys. Rev. B **64**, 184105 (2001).
[9] L. G. Hector, Jr., J. F. Herbst, and T. W. Capehart, J. Alloys Compd. **353**, 74 (2003).
[10] C. Zhang, T. Gao, X. Qi, Y. Zhang, L. Tang, J. Zhou, and B. Chen, Physica B **403**, 2372 (2008).
[11] A. Tezuka, H. Wang, H. Ogawa, and T. Ikeshoji, Phys. Rev. B **81**, 134304 (2010).
[12] H. Nakamura, D. Nguyen-Manh, and D. G. Pettifor, J. Alloys Compd. **281**, 81 (1998).
[13] S. Ishibashi, K. Terakura, and H. Hosono, J. Phys. Soc. Jpn. **77**, 053709 (2008).
[14] P. E. Blöchl, Phys. Rev. B **50**, 17953 (1994).
[15] J. P. Perdew, K. Burke, and M. Ernzerhof, Phys. Rev. Lett. **77**, 3865 (1996).
[16] R. Hempelmann, D. Richter, G. Eckold, J. J. Rush, J. M. Rowe, and M. Montoya, J. Less-Common Met. **104**, 1 (1984).
[17] H. Züchner, T. Rauf, and R. Hempelmann, J. Less-Common Met. **172-174**, 611 (1991).
[18] C. Schönfeld, R. Hempelmann, D. Richter, T. Springer, A. J. Dianoux, J. J. Rush, T. J. Udovic, and S. M. Bennington, Phys. Rev. B **50**, 853 (1994).
[19] D. A. Keen, J. Appl. Crystallogr. **34**, 172 (2001).